CERN-ACC-2019-0030

October 20, 2019

davide.gamba@cern.ch

Update of beam dynamics requirements for HL–LHC electrical circuits

D. Gamba, G. Arduini, M. Cerqueira Bastos, J. Coello De Portugal, R. De Maria, M. Giovannozzi, M. Martino, R. Tomàs Garcia
CERN, CH-1211 Geneva 23, Switzerland

Abstract
Since the publication of the document providing the specifications of the new circuits of the HL–LHC (see [1]), using criteria based on beam dynamics considerations, more accurate expectations of the power converters' performance have been made available. Moreover, cost optimisation and technological considerations on the initially-proposed choices made it necessary a review of the previous document together with clarifications of some details of the previous analysis. The impact on beam parameters of the newly-proposed solutions and new power converter specifications is carried out in this document, and a summary of the new choices is presented.

Keywords
LHC, HL–LHC, circuit specifications, power converters

Contents

1 New Power Converter Uncertainty Specifications

New Power Converter (PC) uncertainty specifications have been defined by the HL–LHC "Warm Powering" Work Package 6B (WP6B) in [2]. The new definitions are reported in the following:

- **Setting resolution**: Smallest step in current that can be induced and discerned.
  - **Units**: Expressed in ppm.
- **Initial uncertainty after calibration**: Deviation of the delivered current with respect to an accepted current reference immediately after calibration.
  - **Conditions**: Frequency range [$1\,\mathrm{mHz}$ - $100\,\mathrm{mHz}$], constant ambient temperature ($\Delta T < 0.1°\mathrm{C}$).
  - **Units, distribution**: Expressed in [$2\times$ rms ppm], Normal distribution.
  - **Notes**: This quantity can be used to estimate the relative error between different circuits.
- **Linearity**: Maximum deviation, in absolute value, of the delivered current from the current reference along the setting range from $-I_{\mathrm{rated}}$ to $0\,\mathrm{A}$ and from $0\,\mathrm{A}$ $+I_{\mathrm{rated}}$ (or from I_{min} to $+I_{\mathrm{rated}}$ for unipolar PCs), corrected for gain and offset.
  - **Conditions**: Average DC value measured after settling time, constant ambient temperature ($\Delta T < 0.1°\mathrm{C}$).
  - **Units, distribution**: Expressed in [$\max\ |.|$ ppm], the linearity of n converters is considered to be uniformly distributed. The value given by this parameter can be interpreted as the maximum (in absolute value) of the uniform distribution.
  - **Notes**: The gain and offset corrections mean that the deviation is zero (within the uncertainty after calibration mentioned above) at $-I_{\mathrm{rated}}$, at $0\,\mathrm{A}$ and at $+I_{\mathrm{rated}}$ (or at I_{min} and at $+I_{\mathrm{rated}}$ for unipolar PCs).
- **Isothermal Stability During a Fill (ISDF) (**$12\,\mathrm{h}$**)**: Variation of the delivered current (for a constant reference) during a period of $12\,\mathrm{h}$, measured up to a frequency of $10\,\mathrm{mHz}$.
  - **Conditions**: Frequency range [$20\,\mu\mathrm{Hz}$ - $10\,\mathrm{mHz}$], constant ambient temperature ($\Delta T = 0°\mathrm{C}$).
  - **Units, distribution**: Expressed in [$\max\ |.|\ \mathrm{ppm}$], the stability of n converters is considered to be uniformly distributed. The value given by this parameter can be interpreted as the maximum (in absolute value) of the uniform distribution.
  - **Notes**: The stability during a $12\,\mathrm{h}$ period is impacted both by drift (due to mechanical stress and environmental effects) and by flicker noise ($1/f$). Since $1/f$ and drift can have similar magnitude over the considered time scale, it was decided for the sake of simplicity, to define the $12\,\mathrm{h}$ stability as a slow and monotonic variation of the delivered current during a fill. It can be either positive or negative, but of constant sign for each power converter.
- **Stability During a Fill (SDF) (**$12\,\mathrm{h}$**)**: same definition as above, but including temperature variation expected in the HL–LHC environment.
- **Stability at the end of the ramp (**$5\,\mathrm{min}$**)**: Variation of the delivered current during a period of $5\,\mathrm{min}$ after a current ramp at nominal speed from zero (or injection current) to the circuit nominal current (I_{nom}).
  - **Conditions**: Frequency range [$20\,\mu\mathrm{Hz}$ - $10\,\mathrm{mHz}$], constant ambient temperature ($\Delta T < 0.1°\mathrm{C}$).
  - **Units, Distribution**: Expressed in [$\max\ |.|\ \mathrm{ppm}$], the stability of n converters is considered to be uniformly distributed. The value given by this parameter can be interpreted as the maximum (in absolute value) of the uniform distribution.

- **Notes**: This parameter is considered to be dominated by thermal settling of the DCCTs in the power converter, after a current step.

- **Isothermal Short Term Stability (ISTS) (**$20\,\mathrm{min}$**)**: Variation of the delivered current (for a constant reference, after the $5\,\mathrm{min}$ interval, discussed above, has elapsed) during a period of 20 minutes, measured up to a frequency of $100\,\mathrm{mHz}$.
  - **Conditions**: Frequency Range [$1\,\mathrm{mHz}$ - $100\,\mathrm{mHz}$], constant ambient temperature ($\Delta T = 0°\mathrm{C}$).
  - **Units, Distribution**: Expressed in [$2\times$ $\mathrm{rms\ ppm}$], the value given by this parameter is based on the rms value of the low-frequency noise (normally distributed) measured during $20\,\mathrm{min}$. Considering there are n converters, the noise to which this rms value refers is the worst case noise amongst n converters measured.
  - **Notes**: This parameter is considered to be dominated by flicker noise ($1/f$).
- **Short Term Stability (STS) (**$20\,\mathrm{min}$**)**: same definition as above, but including ambient temperature variation expected in the HL–LHC environment.
- **Isothermal Fill-to-Fill Repeatability (IFFR)**: Fill-to-fill variation of the average of the delivered current (for a constant reference), measured over 10 consecutive fills.
  - **Conditions**: Measured over 10 consecutive fills, constant ambient temperature ($\Delta T = 0°\mathrm{C}$).
  - **Units, Distribution**: Expressed in [$2\times$ $\mathrm{rms\ ppm}$], the value given by this parameter is based on the rms value of the distribution (assumed Normal) of the averages of 10 fills. Considering there are n converters, the distribution to which this rms value refers is the worst case amongst n converters measured.
- **Fill-to-Fill Repeatability (FFR)**: same definition as above, but including ambient temperature variation expected in the HL–LHC environment.
- **Isothermal Long-Term fill-to-fill Stability (ILTS)**: Variation of the delivered current for the same reference current after one year from the last calibration.
  - **Conditions**: 1 year time span, constant ambient temperature ($\Delta T = 0°\mathrm{C}$).
  - **Units, Distribution**: Expressed in [$\max\ |.|\ \mathrm{ppm}$], the stability of n converters is considered to be uniformly distributed. The value given by this parameter can be interpreted as the maximum (in absolute value) of the uniform distribution.
  - **Notes**: This implies many cycles of the PC. This parameter is dominated, during the first months/years, by ageing of the precision components, which translates into a drift. It is therefore described as a slow and monotonic variation of the delivered current along the year. The direction of the drift varies from PC to PC. Often, drift due to ageing effects (mechanical stress relief) decreases with time and in that case only the flicker noise ($1/f$) and environmental effects remain.
- **Long-Term fill-to-fill Stability (LTS)**: same definition as above, but including ambient temperature variation expected in the HL–LHC environment.
- **Temperature Coefficient (TC) (**$\mathrm{ppm}/°\mathrm{C}$**)**: Dependency of the output current of the PC with ambient temperature.
  - **Units, Distribution**: Expressed in [$\max\ |.|\ \mathrm{ppm}/°\mathrm{C}$], the TC of n converters is considered to be uniformly distributed. The value given by this parameter can be interpreted as the maximum (in absolute value) of the uniform distribution.
  - **Notes**: The expected ambient temperature variations for each PC class are provided separately. For the specific case of the HL–LHC locations, this is provided for the different accuracy classes and is used to calculate the uncertainty for the parameters above which are sizeably effected by temperature: STS, SDF, FFR, LTS, STS.

- **Noise** ($0.1\,\mathrm{Hz}$ **to** $500\,\mathrm{Hz}$): Variation of the delivered current (for a constant reference) within a bandwidth from $0.1\,\mathrm{Hz}$ to $500\,\mathrm{Hz}$.
  - **Conditions**: Frequency Range [$0.1\,\mathrm{Hz}$ - $500\,\mathrm{Hz}$], constant ambient temperature ($\Delta T < 0.1°\mathrm{C}$), measured on a test load (details are clarified in section 1.1).
  - **Units, Distribution**: Expressed in [$2\times$ rms ppm], Normal distribution. Considering there are n converters, the noise to which this rms value refers is the worst case noise amongst n converters measured.
  - **Notes**: This parameter is considered to be a combination of voltage-source noise translated into current according to the load transfer function and white noise originating from the current loop. Since it will be measured on a test load that will, most likely, largely differ from the operational load (magnet), this value cannot be directly used to quantify the noise on the operational circuit, but it requires post-processing (details are clarified in section 1.1).
- **Voltage spectrum tones**: Spectrum line amplitudes at $50\,\mathrm{Hz}$, $150\,\mathrm{Hz}$, $300\,\mathrm{Hz}$ and $600\,\mathrm{Hz}$, f_{sw} and $2\times f_{sw}$, where f_{sw} is the switching frequency (normally of the order of a few kHz) of the power converter [3] (f_{sw} for the HL–LHC and the relevant LHC PCs is reported in Table 4).
  - **Conditions**: $50\,\mathrm{Hz}$, $150\,\mathrm{Hz}$, $300\,\mathrm{Hz}$ and $600\,\mathrm{Hz}$, f_{sw} and $2\times f_{sw}$, constant ambient temperature ($\Delta T < 0.1°\mathrm{C}$).
  - **Units, Distribution**: Expressed in dBµV.
  - **Notes**: These are the most likely tones where to expect voltage ripple, but other tones might appear. In general all tone amplitudes shall be below what specified in the *CERN output ripple limits profile* shown in Fig. 1.

The different quantities are specified in ppm of I_{rated} as rms (with a certain coverage factor normally equal to 2) or as maximum deviation from the reference value.

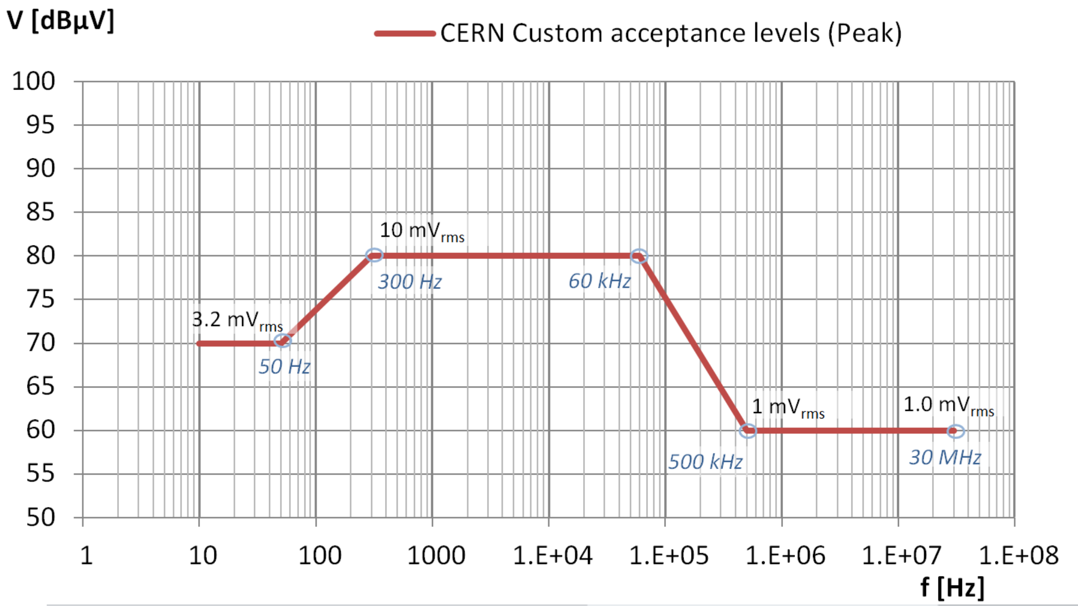

Fig. 1: CERN Output Side Gabarit (< 50 V DC output) [4]. The solid line is the maximum tolerated rms voltage ripple for a given frequency.

The specifications for the different PC classes are detailed in Table 1, together with the maximum ambient temperature variation to be expected in the racks where PCs will be installed for HL–LHC. The

Table 1: New PC class specifications and expected ambient temperature variation for HL–LHC [2].

PC class:	**0**^{a}	**1**^{a}	**2**	**3**	**4**
Setting resolution [ppm]	0.5	0.5	1.0	1.0	1.0
Initial uncertainty after cal. [2$\times$rms ppm]	2.0	2.0	3.0	7.0	10.0
Linearity [$\lvert . \rvert$ max ppm]	2.0	2.0	5.0	8.0	9.0
Isothermal Stability During a Fill (12 h) [max $\lvert . \rvert$ ppm]	0.7^b	1.9^b	5.0	8.0	9.5
Stability at end of ramp (5 min) [max $\lvert . \rvert$ ppm]	0.5	1.5	1.5	3.0	6.0
Isothermal Short Term Stability (20 min) [2$\times$rms ppm]	0.2^b	0.4^b	1.2	2.0	5.0
Noise ($0.1-500$ Hz) [2$\times$rms ppm]	3.0	5.0	7.0	15.0	19.0
Isothermal Fill-to-Fill Repeatability [2$\times$rms ppm]	0.4^b	0.8^b	2.6	4.0	5.0
Isothermal Long Term fill-to-fill Stability [max $\lvert . \rvert$ ppm]	8.0^b	8.0^b	19.0	40.0	45.0
Temperature Coefficient [max $\lvert . \rvert$ ppm/°C]	1.0^b	1.2^b	2.5	5.5	6.5
HL–LHC expected ambient temperature variation (ΔT) [max °C]	0.5	1.0	5.0	5.0	5.0

[a] PC installed in temperature-controlled racks.

[b] An improvement of $1/\sqrt{2}$ should be expected in case the PC is running with regulation loop closed on both DCCT+ADC channels. Such a configuration is expected to be the default in operation, but this is not granted nor insured by TE-EPC/WP6B.

values in Table 1, with the exception of "Noise", are dominated by the current regime performance of the PC. It must be noted that these performance parameters (excluding "Noise") refer to the worst-case scenario of current control loop being "closed" on a single high-precision channel (DCCT + ADC) whereas, in "normal operation", the loop is closed on the average of two channels which would, assuming uncorrelated errors, improve the performance by a factor $1/\sqrt{2}$. Redundancy of the measurement channels is a well-established principle, dating back to LHC design. The specified precision performance is therefore guaranteed even when a channel is recognised as malfunctioning, and hence disabled[1].

The calculation of the uncertainty parameters that include the effect of ambient temperature (i.e. LTS, SDF and FFR) is performed by multiplying the rms of the temperature coefficient by the expected ambient temperature variation, and the resulting value combined in quadrature with the rms of the corresponding isothermal parameter, i.e.:

$$\mathrm{LTS} = 2 \times \sqrt{\left(\Delta T \times \frac{\mathrm{TC}}{\sqrt{3}}\right)^2 + \left(\frac{\mathrm{ILTS}}{\sqrt{3}}\right)^2} \tag{1}$$

$$\mathrm{SDF} = 2 \times \sqrt{\left(\Delta T \times \frac{\mathrm{TC}}{\sqrt{3}}\right)^2 + \left(\frac{\mathrm{ISDF}}{\sqrt{3}}\right)^2} \tag{2}$$

$$\mathrm{FFR} = 2 \times \sqrt{\left(\Delta T \times \frac{\mathrm{TC}}{\sqrt{3}}\right)^2 + \left(\frac{\mathrm{IFFR}}{2}\right)^2} . \tag{3}$$

Note that IFFR is already given in terms of $2\times\mathrm{rms}$, which explains the factor 2 instead of $\sqrt{3}$ in Eq. (3). For the STS, it is assumed that the ambient temperature can be considered constant ($\Delta T \ll 0.1$°C) over 20 minutes, i.e. $\mathrm{STS} = \mathrm{ISTS}$. No assumptions are made on the final distribution since it will be neither uniform nor normal. The final values are computed and summarised in Table 2. Those are also the values that have a direct impact on the slow beam performance in HL–LHC.

1.1 Noise Spectrum

As explained in [2], the PCs work in two different regimes, depending on the frequency range:

[1] Several measures are in place in the PC design to ensure that no failure of the redundant systems remain undetected.

Table 2: New HL–LHC PC specifications, taking into account the expected temperature-induced contributions [2]. Values greater than 5 ppm have been rounded to the closest 0.5 ppm.

PC class:	**0**^{a}	**1**^{a}	**2**	**3**	**4**
Stability During a Fill (12 h) [2×rms ppm]	1.0^b	2.6^b	15.5	33.0	39.0
Stability at end of ramp (5 min) [max $\lvert . \rvert$ ppm]	0.5^b	1.5^b	1.5	3.0	6.0
Short Term Stability (20 min) [2×rms ppm]	0.2^b	0.4^b	1.2	2.0	5.0
Fill-to-Fill Repeatability [2×rms ppm]	0.7^b	1.6^b	14.5	32.0	38.0
Long Term fill-to-fill Stability [2×rms ppm]	9.5^b	9.5^b	26.5	56.0	64.0

[a] PC installed in temperature-controlled racks.

[b] An improvement of $1/\sqrt{2}$ should be expected in case the PC is running with regulation loop closed on both DCCT+ADC channels. Such a configuration is expected to be the default in operation, but this is not granted nor insured by TE-EPC/WP6B.

- **Current source** regime, typically up to a few Hz (for LHC and HL–LHC circuits).
- **Voltage source** regime, above a few Hz (for LHC and HL–LHC circuits).

The frequency range specified in the "Noise" definition covers more than three decades in frequency in which the regime of the converter changes from current to voltage. Table 1 provides guaranteed values for current noise, independently of the regime and measured on a test load. If one were to estimate the noise (0.1 Hz - 500 Hz) to be expected on the operational circuit one should:

1. *measure* (or estimate) the noise spectrum on the test load;
2. *equalise* the measured (or estimated) frequency response of the test load and the expected frequency response of the operational load. The equalisation will not consider the contribution of the regulation algorithm as it is deemed negligible for the vast majority of the considered frequency range;
3. *compute* the rms value from the expected noise spectrum.

Moreover, in order to estimate the impact of high-frequency noise on the beam, one should also consider the current to magnetic field transfer function and its behaviour with frequency. On this subject separate studies [5–8] were carried out and must be carefully considered.

For the reasons exposed above, a decade-by-decade analysis of the converter operation, as exemplified below, might be required:

- **below a few** Hz the converter is likely to be operating within the current regulation loop bandwidth and therefore in a current regime. Noise depends mostly on the power converter's current measurement chain and the regulation loop;
- **above a few** Hz the converter behaves as a voltage source and the current noise is mostly determined by the voltage noise and the nominal inductance and resistance of the load;
- **above a few tens of** Hz voltage tones related to the mains frequency harmonics are likely to be observed. These voltage tones are bounded by the limits given in the CERN output ripple limits profile, shown in Figure 1;
- **above** 100 Hz the effect of the Beam Screen, reported in [5] starts to be non negligible, and current noise does not directly translate into magnetic field noise, as the magnetic field noise is a "low pass" version of the current noise;
- **above a** kHz the effect of losses on the magnets themselves (that comes into play weakly below 100 Hz) starts to provide extra filtering on the conversion from current to magnetic field noise. On the other hand, other voltage tones might show up, such as the power converter switching frequency

harmonics (Reported in Table 4). It should also be noted that resonances cannot be excluded for frequencies above $1\,\text{kHz}$ due to parasitic capacitance of magnets and/or (cold) diodes connected in parallel for protection purposes. The impact of such resonances should be investigated in a dedicated study.

A detailed "decade-by-decade" study will be carried out and reported in an upcoming note.

For the time being, assuming that the "Noise" values from Table 1 would affect the beam without any reduction, the beam stability figures in the $0.1 - 500\,\text{Hz}$ range would be those reported in Table 3. It is important to stress that those are expected to be upper bound and pessimistic values, which should not be used to draw predictive conclusions. On the other hand, one should expect that part of this "Noise" might affect the precision of K-modulation measurements used to measure and correct β^*. Further investigations on the behaviour of the PCs and relative circuits in this frequency range is therefore necessary.

Table 3: Simulated HL–LHC stability figures corresponding to the "Noise" values from Table 1 (15 cm β^* nominal optics HLLHCV1.3).

Tune stability [rms]	Orbit stability [rms]	Beta Beating [rms]
5×10^{-4}	$3\%\ \sigma_{\text{beam}}$	3×10^{-3}

Table 4: Switching frequencies of PCs for HL–LHC circuits. A range is given for new PCs for which the actual switching frequency is still unknown.

Circuit name	I_{rated} **[A]**	**PC class**	f_{sw} **[kHz]**
RB[ab]	13000	1	n.a.[b]
RQ(D/F)[a]	13000	1	25
RQX	18000	0	$20 \div 200$
RTQX1	2000	2	50
RTQXA1	60	4	$45 \div 200$
RTQX3	2000	2	50
RCBX	2000	2	50
RQSX	600	3	50
RC(S/O)X	120	4	$45 \div 200$
RC(D/T)X	120	4	$45 \div 200$
RD(1/2)	14000	0	50
RCBRD	600	3	50
RQ4[a]	4000	2	50
RQ(5/6)[a]	5000	2	50
RCBY[a]	120	4	$50 \pm 10\%$
RCBC[a]	120	4	$50 \pm 10\%$
RTBH9	600	3	50

[a] Existing circuit assumed not to be upgraded.

[b] Main dipole PCs are based on thyristors technology, which is fundamentally different than Switch Mode Power Supply (SMPS) technology used for the other PCs. Its first tone is expected to be around $600\,\text{Hz}$.

2 On-Demand PC Calibration

In order to simplify the installation and to allow for a reduction of material cost, it is agreed not to install a remote calibration system for class 0 converters. However, in case of suspected loss of performance, it is agreed that EPC will carry out the necessary verification and calibration of specific class 0 converters on demand during a technical stop. This will allow to improve the value of LTS.

3 Proposed PC Classes for HL–LHC Circuits and Expected Beam Stability

The choice of PC classes remains unchanged with respect to [1], however their specification and therefore the impact on the beam had to be updated.

The proposed classes for each main HL–LHC circuit are summarised in Table 5, together with the most relevant updated specification from Table 2.

Table 5: Amended proposal of PC class for HL–LHC circuits. All uncertainties are given as $2\times$ ppm rms of I_{rated} and include the expected temperature-drift effect in HL–LHC.

Circuit name	I_{rated} [A]	PC class	Short Term Stability	Stability During a Fill (12 h)	Long Term fill-to-fill Stability
RB[a]	13000	1	0.4	2.6	9.5
RQ(D/F)[a]	13000	1	0.4	2.6	9.5
RQX	18000	0	0.2	1.0	9.5
RTQX1	2000	2	1.2	15.5	26.5
RTQXA1[b]	60	4	5.0	39.0	64.0
RTQX3	2000	2	1.2	15.5	26.5
RCBX	2000	2	1.2	15.5	26.5
RQSX[d]	600	3	2.0	33.0	56.0
RC(S/O)X	120	4	5.0	39.0	64.0
RC(D/T)X	120	4	5.0	39.0	64.0
RD(1/2)	14000	0	0.2	1.0	9.5
RCBRD	600	3	2.0	33.0	56.0
RQ4[a]	4000	2	1.2	15.5	26.5
RQ(5/6)[a]	5000	2	1.2	15.5	26.5
RCBY[a]	120	4	5.0	39.0	64.0
RCBC[a]	120	4	5.0	39.0	64.0
RTBH9[c]	600	3	2.0	33.0	56.0

[a] Existing circuit assumed not to be upgraded.
[b] The proposed value is compatible with the use of the trim as $I_{\mathrm{max}} = 35$ A in operation.
[c] A standard 600 A PC of class 3 is assumed even though $I_{\mathrm{max}} = 250$ A in operation.
[d] A standard 600 A PC of class 3 is assumed even though $I_{\mathrm{max}} = 200$ A in operation.

Table 6 shows different values of tune stability considering the specifications over different time scales as presented in Table 5. Similarly, Table 7 shows the expected β^* stability and Table 8 shows the expected orbit stability at IP1 and IP5. All values have been computed for the HL–LHC optics version 1.3 for Beam 1, which is assumed to be representative also for Beam 2. The circuits that have the strongest impact on beam performance remain the main dipoles, main quadrupoles, and triplets in IR1 and IR5, as already discussed in [1]. The impact of D1 and D2, matching section quadrupoles, linear and non-linear IT correctors, and orbit correctors up to Q6 around IP1 and IP5 have also been included in the computation. It is expected that all other circuits have a much smaller or negligible contribution. It was also assumed that all circuit are independent from each other, i.e. their contributions have been summed up in quadrature. Note that an improvement of up to a factor $1/\sqrt{2}$ could be obtained if all PCs would run profiting of the redundancy of their DCCT and ADC measurement systems.

Table 6: Simulated HL–LHC Beam 1 tune stability (15 cm β^* nominal optics HLLHCV1.3). The "Old" beam stability estimates refer to the previous performance specifications as mentioned in [1].

	Tune jitter [10^{-5} rms]					
	20min.		**12h fill**		**Long term**	
	Old	**New**	**Old**	**New**	**Old**	**New**
x	4.1 (2.8^+)	4.1 (2.9^+)	23.9	30.7	138	114
y	4.1 (2.8^+)	4.1 (2.9^+)	23.4	30.3	135	112
Target		< 1		n.a.		n.a.

$^+$ Assuming to upgrade arc dipoles in sectors 8–1, 1–2, 4–5, 5–6 to class 0.

Table 7: Simulated HL–LHC Beam 1 β^* stability in IP1/IP5 (15 cm β^* nominal optics HLLHCV1.3). The "Old" beam stability estimates refer to the previous performance specifications as mentioned in [1].

	$\Delta\beta^*/\beta^*_0$ [10^{-3} rms]					
	20min.		**12h fill**		**Long term**	
	Old	**New**	**Old**	**New**	**Old**	**New**
IP1 H	0.2 (0.1^+)	0.2 (0.1^+)	1	1	5	5
IP1 V	0.1 (0.1^+)	0.1 (0.1^+)	1	1	4	4
IP5 H	0.2 (0.1^+)	0.2 (0.1^+)	1	1	7	6
IP5 V	0.1 (0.1^+)	0.1 (0.1^+)	1	1	5	4

$^+$ Assuming to upgrade arc dipoles in sectors 8–1, 1–2, 4–5, 5–6 to class 0.

Table 8: Simulated HL–LHC Beam 1 orbit stability in IP1/IP5 (15 cm β^* nominal optics HLLHCV1.3). The "Old" beam stability estimates refer to the previous performance specifications as mentioned in [1].

	$\Delta(x^*\|y^*)$ [10^{-2} σ_{beam} rms]					
	20min.		**12h fill**		**Long term**	
	Old	**New**	**Old**	**New**	**Old**	**New**
IP1 H	0.3 (0.2^+)	0.3 (0.3^+)	1.3	2.7	8.8	8.5
IP1 V	0.2 (0.2^+)	0.2 (0.2^+)	1.1	2.3	6.2	4.7
IP5 H	0.3 (0.3^+)	0.3 (0.3^+)	1.8	2.8	11.2	9.2
IP5 V	0.2 (0.2^+)	0.2 (0.2^+)	1.2	2.3	6.4	4.8

$^+$ Assuming to upgrade arc dipoles in sectors 8–1, 1–2, 4–5, 5–6 to class 0.

3.1 Impact on Flat Optics

Another question is the performance of flat optics. Tables 9, 10, 11 show the difference in performance between the nominal 15 cm β^* nominal round optics and the presently most demanding (non baseline) 7.5-18 cm β^* flat optics considering the PC specifications from Table 5.

Table 9: Simulated HL–LHC Beam 1 tune stability: 15 cm β^* round vs 7.5-18 cm β^* optics (HLLHCV1.3).

	Tune jitter [10^{-5} rms]					
	20min.		12h fill		Long term	
	15 cm	7.5 cm	15 cm	7.5 cm	15 cm	7.5 cm
x	4.1 (2.9$^+$)	6.3 (4.2$^+$)	30.7	47.0	114	175
y	4.1 (2.9$^+$)	6.1 (4.1$^+$)	30.3	45.8	112	170
Target	< 1		n.a.		n.a.	

$^+$ Assuming to upgrade arc dipoles in sectors 8–1, 1–2, 4–5, 5–6 to class 0.

Table 10: Simulated HL–LHC Beam 1 β^* stability in IP1/IP5: 15 cm β^* nominal round vs 7.5-18 cm β^* optics (HLLHCV1.3).

	$\Delta\beta^*/\beta^*_0$ [10^{-3} rms]					
	20min.		12h fill		Long term	
	15 cm	7.5 cm	15 cm	7.5 cm	15 cm	7.5 cm
IP1 H	0.2 (0.1$^+$)	0.2 (0.1$^+$)	1	2	5	6
IP1 V	0.1 (0.1$^+$)	0.2 (0.2$^+$)	1	2	4	6
IP5 H	0.2 (0.1$^+$)	0.4 (0.3$^+$)	1	3	6	10
IP5 V	0.1 (0.1$^+$)	0.2 (0.1$^+$)	1	1	4	5

$^+$ Assuming to upgrade arc dipoles in sectors 8–1, 1–2, 4–5, 5–6 to class 0.

Table 11: Simulated HL-LHC Beam 1 orbit stability in IP1/IP5: 15 cm β^* round vs 7.5-18 cm β^* optics (HLLHCV1.3).

	$\Delta(x^*\|y^*)$ [10^{-2} σ_{beam} rms]					
	20min.		12h fill		Long term	
	15 cm	7.5 cm	15 cm	7.5 cm	15 cm	7.5 cm
IP1 H	0.3 (0.3$^+$)	0.3 (0.3$^+$)	2.7	3.0	8.5	9.7
IP1 V	0.2 (0.2$^+$)	0.3 (0.3$^+$)	2.3	2.7	4.7	5.1
IP5 H	0.3 (0.3$^+$)	0.4 (0.4$^+$)	2.8	3.4	9.2	10.9
IP5 V	0.2 (0.2$^+$)	0.3 (0.3$^+$)	2.3	2.7	4.8	5.1

$^+$ Assuming to upgrade arc dipoles in sectors 8–1, 1–2, 4–5, 5–6 to class 0.

4 Separation Orbit Collapse Speed

Another aspect to clarify is the speed of the orbit bump collapse to go into collision. The orbit corrector strength required to implement ± 0.75 mm orbit separation at IP1/5 are summarised in Table 12, together with the main characteristic of the associated orbit corrector magnets and the requested speed and acceleration rates requested in [1]. Note that the requested speed and acceleration rates in Table 12 have been driven by orbit correction considerations, and not by the speed of the orbit separation collapse. As in [1], the requirement for the speed of beam separation collapse remains the same, i.e. to go from 2 to 0 σ_{beam} total separation in less than 3 s [10, 11]. Assuming $\epsilon_{\mathrm{n}} = 2.5$ μm and the worst case $\beta^* = 70$ cm, then the value of ± 0.75 mm associated to the separation knob presented in Table 12 corresponds to about $49\sigma_{\mathrm{beam}}$ [1]. Figure 2 shows the time evolution of the half beam separation when considering either the specification or the fastest collapse considering the limits specified in Table 12. The actual maximum

Table 12: Necessary integrated strength to implement the orbit separation (± 0.75 mm) knob for IP1/5 at 7 TeV [9]; max strength and current of the associated orbit corrector magnets [9] and their nominal speed and acceleration rates [1].

Circuit name	**Half-separation [Tm]**	$\int B_{\rm nom}$**d**l **[Tm]**	$I_{\rm nom}$ **[A]**	**Ramp rate [A/s]**	**Acceleration [A/s^2]**
RCBX1	0.08	2.5	1600	15	5
RCBX2	0.08	2.5	1600	15	5
RCBX3	0.20	4.5	1600	15	5
RCBRD4	0.10	5	430	2	1
RCBY4	0.02	2.79	88	0.67	0.25

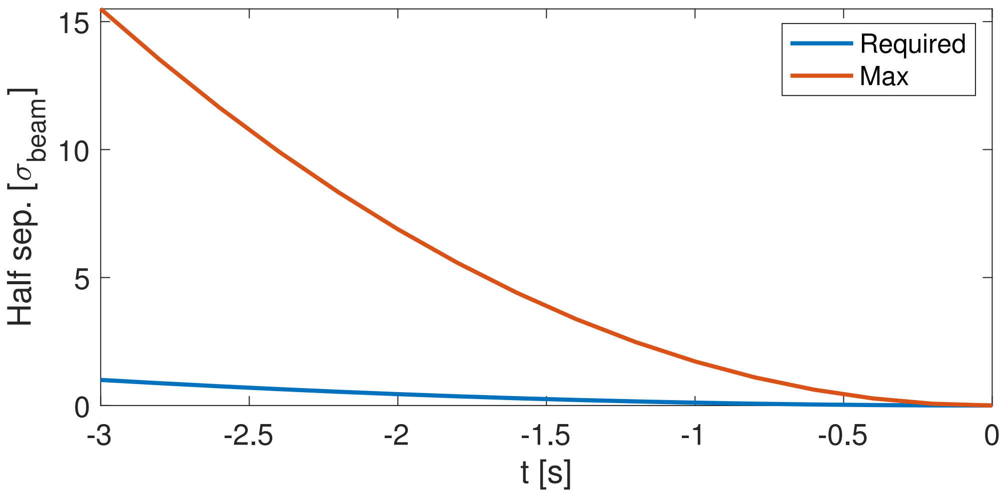

Fig. 2: Half separation in beam sigma (assuming $\epsilon_{\rm n} = 2.5$ μm and $\beta^* = 70$ cm) as a function of time during possible implementations of the orbit-separation collapse.

speed and acceleration exploited during the two versions of orbit collapse are summarised in Table 13. The total time necessary for the collapse is 74 s and 7 s for the required and fastest collapse, respectively.

5 Conclusions

New definitions and specification for the PCs have been defined based on [2]. The difference in expected beam stability with respect to [1] turned out to be minimal, therefore no change of choice of PC classes have been made. It is also confirmed that an on-demand remote calibration system for class 0 PCs is not necessary to guarantee safe and continuous beam operation during a year. However, the possibility of performing manual calibration on-request during a technical stop is kept in case of evident degradation of the beam performance.

It should be noticed that the 10^{-5} tune-stability requirement for ensuring optics control for the lowest β^* optics in HL–LHC is still to be met [12]. With the present knowledge, a possible, but expensive, improvement consists of upgrading to class 0 the main dipole PCs for the ATS arcs. Such an upgrade is presently not foreseen in the HL–LHC baseline, and its implementation should be evaluated

Table 13: Required and maximum speed and acceleration for the orbit separation collapse shown in Figure 2.

Circuit name	**Ramp rate [A/s]**		**Acceleration [A/s^2]**	
	Required	**Max**	**Required**	**Max**
RCBX1	0.70	10.8	0.23	3.6
RCBX2	0.70	10.8	0.23	3.6
RCBX3	0.97	15	0.32	5
RCBRD4	0.12	1.81	0.04	0.60
RCBY4	0.01	0.13	<0.01	0.04

and discussed in the early phase of HL–LHC. Moreover, one might profit of an improvement factor, up to $1/\sqrt{2}$, with respect to the class 0 and class 1 PC specifications due to the presence of two redundant and independent DCCT+ADC measurement channels. This would be available at no extra cost, but it still needs to be verified (as this is not guaranteed by the present operational strategy for the PCs).

On the other hand, there is still no accurate estimation of the magnetic field fluctuation induced by the PC at frequencies above $0.1\,\mathrm{Hz}$ generated by the PC in voltage-control regime. The PC "Noise" specification currently provided should cover this regime, but it cannot be directly applied to estimate the impact on the beam, also due to several damping effects. A detailed study of this regime must be carried out, especially to verify that this does not further deteriorate the accuracy of the K-modulation measurements used to measure and correct for β^* errors.

As a separate topic, it has been verified that the IP orbit-separation collapse can be executed much faster than required by beam stability considerations. In fact, the speed and acceleration requirements for the orbit corrector circuits are dominated by more demanding considerations on general orbit correction, which were already discussed in [1].

References

[1] D. Gamba, G. Arduini, M. Cerqueira Bastos, J. M. Coello De Portugal Martinez Vazquez, R. De Maria, M. Giovannozzi, M. Martino, and R. Tomas Garcia, "Beam dynamics requirements for HL–LHC electrical circuits," Dec 2017.

[2] M. Cerqueira Bastos and M. Martino, "HL–LHC Power Converters Requirements," Tech. Rep. EDMS n. 2048827 v.1, CERN, Geneva, 2018.

[3] M. Cerqueira Bastos. Private Communication.

[4] "CERN TE-EPC-LPC Converter-Concepts / EMC." `http://te-epc-lpc.web.cern.ch/te-epc-lpc/concepts/converters/emc/emc_emissions.stm`, August 2017.

[5] M. Morrone, M. Martino, R. De Maria, M. Fitterer, and C. Garion, "Magnetic frequency response of high-luminosity large hadron collider beam screens," *Phys. Rev. Accel. Beams*, vol. 22, p. 013501, Jan 2019.

[6] M. Martino, "MQXFS-5 Warm and Cold Measurement Test Report," Tech. Rep. EDMS n. 1843088 v.1, CERN, Geneva, 2017.

[7] M. Martino, "Modelling of the PC Output to the Magnetic Field," in *HL-MCF Meeting #7*, November 2016. `https://indico.cern.ch/event/580993/contributions/2355718/`.

[8] M. Martino, "Admittance model for (superconducting) magnets for power converters control," Tech. Rep. EDMS n. 2032753 v.1, CERN, Geneva, 2017.

[9] R. De Maria, "Follow-up on orbit corrector requirements for IP and crab-cavity alignment," in *81st HiLumi WP2 Meeting*, November 2016. `https://indico.cern.ch/event/572438/`

contributions/2379420/.

[10] C. Tambasco, "Specification of separation collapsing speed," in *67th HiLumi WP2 Meeting*, April 2016. https://indico.cern.ch/event/512381/contributions/2146006/.

[11] R. De Maria, "Specification of separation collapsing speed," in *Joint LARP CM26/Hi-Lumi Meeting at SLAC*, May 2016. https://indico.fnal.gov/event/11049/session/5/contribution/55.

[12] R. Tomás *et al.*, "LHC Run 2 Optics Commissioning Experience in View of HL–LHC," in *Proceedings of the 10th International Particle Accelerator Conference, IPAC19*, (Melbourne, Australia), p. MOPMP033, May 2019.